AIMS Bioengineering

AIMS Bioengineering, 12(3): 435–452.
DOI: 10.3934/bioeng.2025021
Received: 09 July 2025
Revised: 01 September 2025
Accepted: 08 September 2025
Published: 12 September 2025

https://www.aimspress.com/journal/Bioengineering

Research article

A study on the restoration strategy of a four-unit bridge in the anterior region: a finite element analysis

Song Huang[1], Jianguo Zhang[1,*], Xiaoying Zhang [2,*], Fengling Hu[3,4,*] and Youcheng Yu[4]

[1] Faculty of Intelligence Technology, Shanghai Institute of Technology, No. 100 Haiquan Road, Shanghai 201418, China
[2] Department of Stomatology, The Fifth People's Hospital of Shanghai, Fudan University, No. 801, Heqing Road, Minhang District, Shanghai 200240, China
[3] Department of Stomatology, Shanghai Geriatric Medical Center, No. 2560, Chunshen Road, Minhang, Shanghai 200240, China
[4] Department of Stomatology, Zhongshan Hospital, Fudan University, No. 180, Fenglin Road, Xuhui, Shanghai 200032, China

* **Correspondence:** Email: jgzhang98328@163.com; zhangxiaoying_32@163.com; flhu201418@163.com.

Abstract: This study evaluated the feasibility of cantilever and fixed bridge restorations through finite element analysis of narrow-diameter implants (NDIs) in a 4-unit anterior mandibular bridge. A total of five restoration models were analyzed using static, modal, and dynamic analyses. Results showed that the fixed bridge supported by three NDIs exhibited the lowest stress (crown: 27.429 MPa, implant: 58.608 MPa) and optimal stability (resonance frequency: 8653 Hz). The maximum stresses in cantilever bridge implants (crowns: 78.803 MPa, implants: 146.27) were 2–3 times higher than those in fixed bridges. Dynamic loading generated the highest stresses during the second phase of the masticatory cycle, with overall stress 10%–30% higher than under static loading. Fixed bridges supported by three NDIs are recommended for optimal stress distribution, while cantilever bridges should be used with caution.

Keywords: four-unit bridge; NDIs; cantilever bridge; fixed bridge; finite element analysis

1. Introduction

Dental implants have become the mainstream restoration option for patients with missing teeth, accompanied by technological development, with a success rate of over 90% after years of research [1]. Dental implants have the advantages of high chewing efficiency, strong stability, natural appearance, and long service life. Despite their mature development, certain difficulties remain in the oral environment of the anterior tooth area [2]. Due to anatomical constraints and aesthetic requirements, the absence of multiple incisors in the anterior dental area typically results in a thin and easily resorbed buccal bone plate, hard bone, poor blood supply conditions, and narrow implant spacing [3]. Conventional bone augmentation techniques have difficulty in their implementation, whereas NDIs offer apparent advantages in the anterior tooth area and are comparable to traditional implants. This has been confirmed by a growing number of scholars through experimental data analysis. Telles [4] conducted a meta-analysis and found no difference between the success rates of NDIs and standard-diameter implants (SDIs) during a follow-up period of up to 3 years. González-Valls [5] included 15 studies with 1245 implants through meta-analysis. The results showed that the survival rate of NDIs was 97%, with no significant difference compared with SDIs. Therefore, NDIs have become the mainstream choice for anterior tooth restoration.

Fixed bridge implants are commonly used in current clinical practice; another type of cantilever bridge restoration is also noteworthy. Cantilever restorations offer excellent advantages in cases of poor bone conditions. Using a cantilever bridge restoration, bone defect areas can be effectively avoided and the problem of narrow spacing can be solved, thereby maximizing the protection of soft tissues, reducing surgical trauma, and lowering surgical costs [6,7]. However, the impact of its stress concentration should not be ignored. Zhang et al. [8] simulated the fixed bridge implant restoration and cantilever bridge implant restoration in the maxillary incisor region using a three-dimensional finite element method, applying loads in the 0°, 30°, and 60° directions. They found stress concentration in the cantilever bridge, making it not recommended. Valera-Jiménez et al. [9] compared single-implant, three-unit, and four-unit bridge restorations using finite element analysis and found that the cantilevered structures generated increased compressive stresses around the implants. However, there is controversy over the repair plans for fixed bridges and cantilever bridges. Through static analysis, Sadek et al. [10] evaluated the mechanical properties of cantilevered two-unit implants made of two materials under three loading conditions. The results showed that zirconia implants can effectively resist bending stress, and the maximum equivalent stress generated by cantilevered implants is much lower than the yield limit of the material. Zirconia is therefore more suitable for cantilevered design. Kondo et al. [11] conducted a meta-analysis, including nine eligible studies (such as implant survival rate), and found no adverse effects of cantilever implants on implant survival rate, marginal bone loss, and patient satisfaction. Fixed bridges and cantilever bridges based on NDIs remain challenging in the anterior region.

Since the mandibular anterior region is an anatomically restricted area, clinicians are commonly limited in selecting implant restorations based on empirical judgment. NDIs are currently studied through meta-analysis and clinical applications, lacking theoretical research from a biomechanical perspective. Furthermore, static loading methods are mostly used, while the real chewing is a dynamic process; this highlights the need for dynamic analysis [12–16]. To solve the above problems, this paper conducted a comprehensive comparative analysis of various restorative modalities for four missing incisors in the mandibular region from a biomechanical perspective using finite element

static, modal, and dynamic analyses, aiming to explore the restorative scheme with optimal mechanical performance and provide biomechanical guidance for clinicians in selecting restorative schemes in anatomically restricted areas.

2. Methods

2.1. Finite element modeling

A healthy volunteer with complete dentition, no deformities, and no jawbone disease was selected for CBCT scanning, and the resulting data were saved in DICOM format. The volunteer provided informed consent, and this study was approved by the Medical Ethics Committee of Zhongshan Hospital, Fudan University, with approval number B2024-068R. The CBCT image was imported into Mimics Research 21.0 software, and the jawbone, teeth, and soft tissues were extracted using grayscale values. The mask was edited in multiple layers, holes were filled, preliminary smoothing was performed, and the object was solidified and saved in STL format. The model was then imported into Geomagic Studio 2021 software for local feature processing, smoothing the surface and obtaining an accurate mandible model through precise surface modeling and extraction of the anterior tooth area. Referring to the Astra Tech Implant System EV implant parameters, SolidWorks 2021 was used to create a 3 × 13 mm narrow-diameter implant and related abutments and screw accessories, so as to ensure a perfect mechanical fit. All models were assembled using the origin constraint in SolidWorks to achieve the actual model effect, as shown in Figure 1.

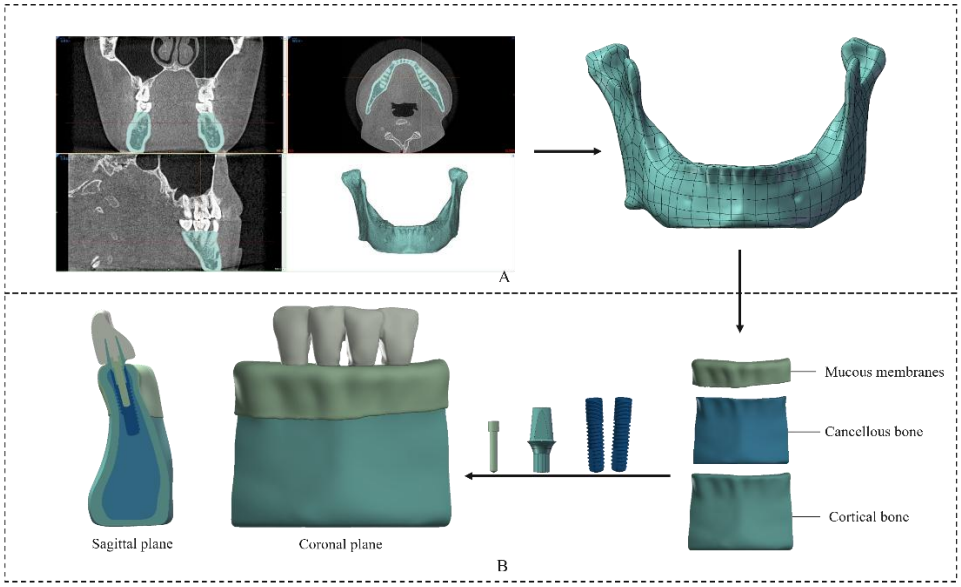

Figure 1. Steps in the finite element modeling process for mandibular implant restoration. A) Reverse modeling to extract the mandible. B) Model assembly.

A total of five groups of models were set up for this experiment: a double-end cantilever bridge supported by two implants (M1), a single-end cantilever bridge supported by two implants (M2), a fixed bridge supported by two implants (M3), a single-end cantilever bridge supported by three implants (M4), and a fixed bridge supported by three implants (M5), as shown in Figure 2.

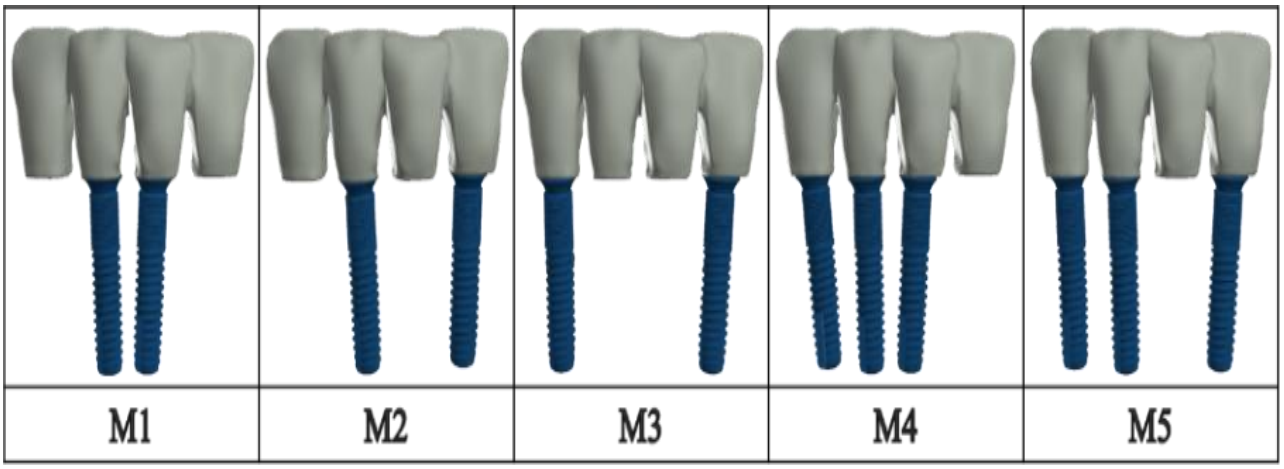

Figure 2. Five implant restorations for four consecutively missing teeth.

2.2. Material properties

Ansys Workbench 2021 software was used for the simulation. The geometric model material properties during preprocessing are shown in Table 1. The bone in the mandibular anterior region is relatively complex, typically classified as Type I or Type II bone. In this study, Type II cancellous bone was used. The tooth crown is made of zirconia, while the implant, abutment, and screw are all medical-grade Ti6Al4V. All materials are assumed to be continuous, homogeneous, and linearly elastic. Cortical bone and cancellous bone are orthotropic, while the remaining materials are isotropic. A 100% osseointegration was assumed between the implant and the surrounding bone. The secondary stability of the implant and the surrounding bone was explored [17,18].

Table 1. Material properties.

Materials	Modulus of elasticity/MPa	Poisson's ratio		References
Cortical bone	E_{xx} 12600	ν_{xy} 0.3	ν_{yx} 0.3	[19]
	E_{yy} 12600	ν_{yz} 0.253	ν_{zy} 0.39	
	E_{zz} 19400	ν_{xz} 0.253	ν_{xz} 0.39	
Cancellous bone	E_{xx} 1148	ν_{xy} 0.055	ν_{yx} 0.01	[19]
	E_{yy} 210	ν_{yz} 0.01	ν_{zy} 0.055	
	E_{zz} 1148	ν_{xz} 0.322	ν_{zx} 0.322	
Zirconium dioxide	210000	0.30		[20]
Ti-6Al-4V	110000	0.35		[20]
Periodontium	6850	0.45		[21]

2.3. Boundary conditions

For each group of models, the side surface of the cortical and cancellous bones was used as the fixation surface. The implants were fixed to the central screw with a friction contact coefficient of 0.3. The tightening torque of the screw and the implant was 15 Ncm and 35 Ncm, respectively, thereby simulating a realistic contact [22]. Static simulation of maximum chewing stress will be loaded vertically in the median part of the four incisors. According to the average chewing force range of 30–300 N in China's standards, the loaded force should be 150 N [23]. Although the transient analysis is a real simulation of a cycle of oral chewing, this paper used a dynamic chewing cycle of 0.875 s. Dynamic loading was divided into five stages, mainly vertical load and inclined load, with a total force of 150 N applied to the median part of the four incisors. The specific loading time, location, and angle are shown in Table 2, and the location and direction of the load are shown in Figure 3(b).

Table 2. Loading conditions during one chewing cycle [24].

Loading time	Loading position	Force (N)	Loading direction
I: 0.000–0.130 s	—	—	—
II: 0.130–0.150 s	The center of the tooth tip	150	Vertically downward with the jaw
III: 0.150–0.260 s	The side edge of the tip of the tooth	150	The lip is inclined downward at an angle of 30° to the crown surface
IV: 0.260–0.300 s	The side edge of the tip of the tooth	150	Tongue deviates downward and forms a 30° angle with the coronoid surface
V: 0.300–0.875 s	—	—	—

2.4. Mesh convergence

The model was successively divided into meshes. It is more reasonable to use C3D10 tetrahedral elements, as most of the area is curved. The mesh was analyzed for convergence by changing the element size. The relative deviation value for convergence was calculated using the following formula:

$$E_r = \left|V_2 - V_1\right| / V_1 \times 100\% \quad (1)$$

Where E_r is the relative error, V_1 is the stress value corresponding to the first division of the grid, and V_2 is the stress value corresponding to the second subdivision of the grid. Generally, the relative stress deviation between the implant and the cortical bone is less than 5% between two consecutive meshes, and meshes are considered converged [25]. The convergence results are shown in Table 3 and Table 4. As shown in Figure 3(a), the meshing size of the implant and accessories, as well as the cortical and cancellous bones, is 0.1 and 0.4 mm, respectively. The calculated model has about 2 million elements and 3.5 million nodes.

Table 3. Mesh convergence results for implant.

Mesh size (mm)	Implant von mises stress (MPa)	Relative error (%)
0.4	123.5	-
0.3	133.5	8.1
0.2	140.4	5.2
0.1	146.3	4.2

Table 4. Mesh convergence results for cortical bone

Mesh size (mm)	Maximum principal stress of cortical bone (MPa)	Relative error (%)
0.7	13.1	-
0.6	14.2	8.4
0.5	15.0	5.6
0.4	15.7	4.7

2.5. Static analysis

Static analysis simulates the static effects of maximum masticatory force. This paper primarily investigated the influence of stress distribution on the crown, implant, and surrounding bone tissue. The von Mises stress criterion is commonly used to evaluate plastic materials, while the maximum principal stress criterion is used to evaluate brittle materials. In this experiment, the von Mises equivalent stress criterion was used to assess the stress distribution of the crown and implant, while the maximum principal stress criterion and Frost's minimum strain stimulation theory were used to evaluate the stress and strain distribution in cortical bone and cancellous bone [26,27].

2.6. Modal analysis

Modal analysis was conducted on the five models on their sixth-order resonance frequencies, and maximum deformation was used as the output. Modal analysis can identify the natural frequencies of the entire implant system and understand at what frequency the entire implant system will resonate, which is typically related to the mass characteristics and boundary conditions of the system.

2.7. Transient analysis

Conventional integration schemes mainly incorporate direct integration and modal superposition methods to ensure the convergence of transient analysis during post-processing. Considering the nonlinear contact effect between the implant and cancellous bone, the Newmark direct integration method was used. Its recursive formula for calculating the displacement and acceleration of $t_{n+1} = t_n + \Delta t$ is:

$$\begin{aligned} \dot{u}_{n+1} &= \dot{u}_n + (1-\gamma)\Delta t\ddot{u}_n + \gamma\Delta t\ddot{u}_{n+1} \\ u_{n+1} &= u_n + \Delta t\dot{u}_n + (0.5-\beta)\Delta t^2\ddot{u}_n + \beta\Delta t^2\ddot{u}_{n+1} \end{aligned} \tag{2}$$

When the time step is small enough, it can converge. Therefore, we enabled the automatic time step and set the step size to 0.01 s [28,29]. We activated dynamic friction contact and then set the

friction coefficient μ to 0.3 and the contact separation threshold to 0.1 mm using Coulomb's law of friction. The calculation formula is as follows:

$$F_t = \mu F_n \tag{3}$$

Where F_n is the normal component contact force, and F_t is the tangential component contact force. During the dynamic chewing process, the contact force between each node is the resultant of tangential and normal components, and the contact force generated by each node at the tooth tip contact interface is equivalent to the actual chewing force. The results were analyzed using the same stress evaluation criteria as in statics.

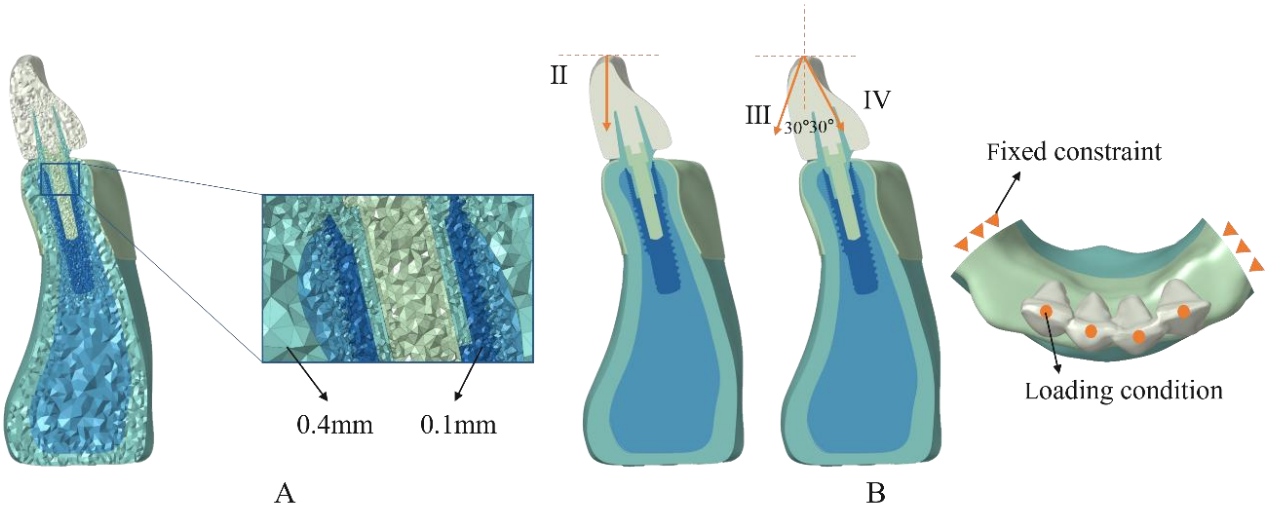

Figure 3. Meshing, constraints, and loading conditions. A) Mesh size setting. B) Constraints and loading conditions.

3. Results

In static analysis, as shown in Figure 4, M1 exhibited the highest crown von Mises stress and implant von Mises stress compared with other groups. The maximum von Mises stress of the crown and the implant was 78.803 and 146.27 MPa, respectively. In contrast, M5 had the lowest von Mises stress values, with a minimum von Mises stress of the crown and the implant being 27.429 and 58.608 MPa, respectively. Notably, the maximum principal stresses in cortical and cancellous bones also exhibited a similar pattern. Additionally, the maximum principal strain was 1287 με in M5 and 3,568 με in M1 (almost three times that of M5), indicating that the design of the cantilever bridge can cause severe stress concentration.

In modal analysis, as shown in Figure 5, the sixth-order mode was mainly analyzed in the modal analysis. It can be seen that the resonance frequency of each order increased with the mode shape. The first-order resonance frequency of M1 was 325 Hz, while the sixth-order resonance frequency was 5473 Hz. The overall resonance frequency was the smallest in M1 and the largest in M5 (a maximum of 8653 Hz).

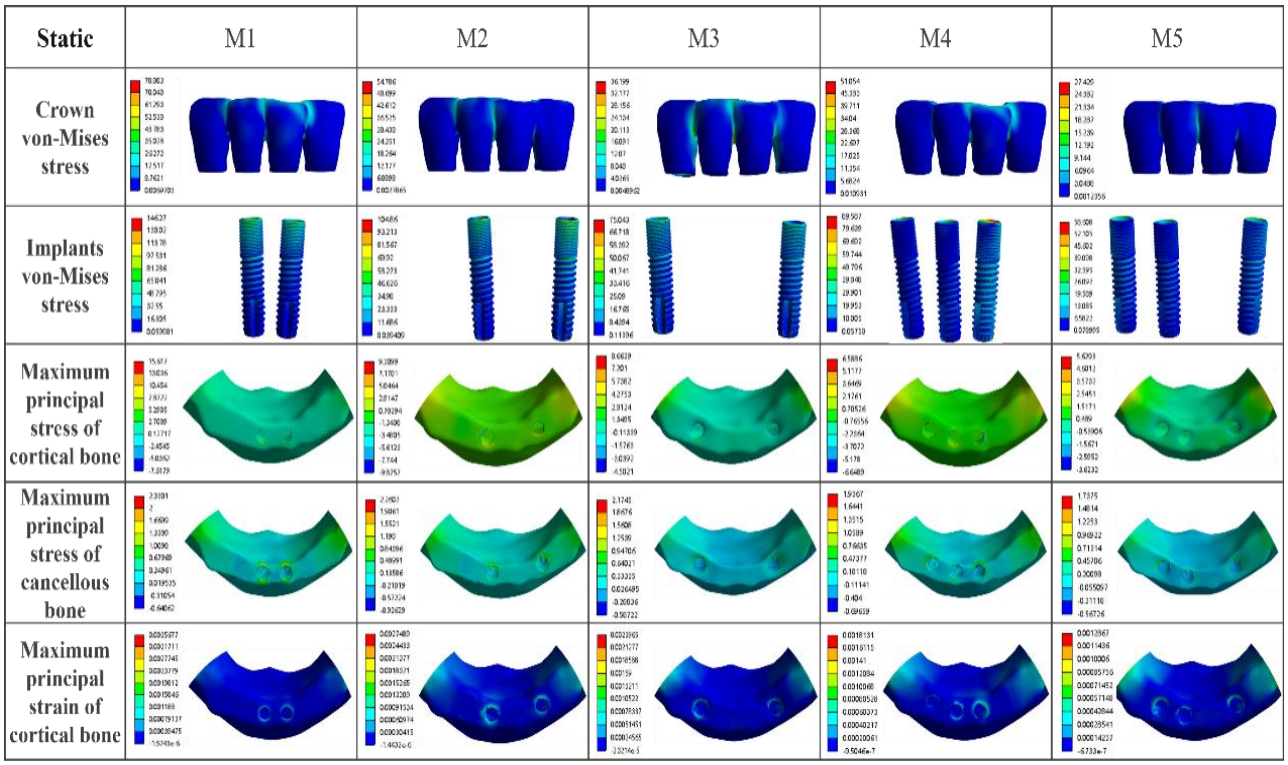

Figure 4. Representative screenshots of static analysis results (crown and implants von Mises stress, maximum principal stress of cortical bone and cancellous bone, and maximum principal strain of cortical bone for M1–M5).

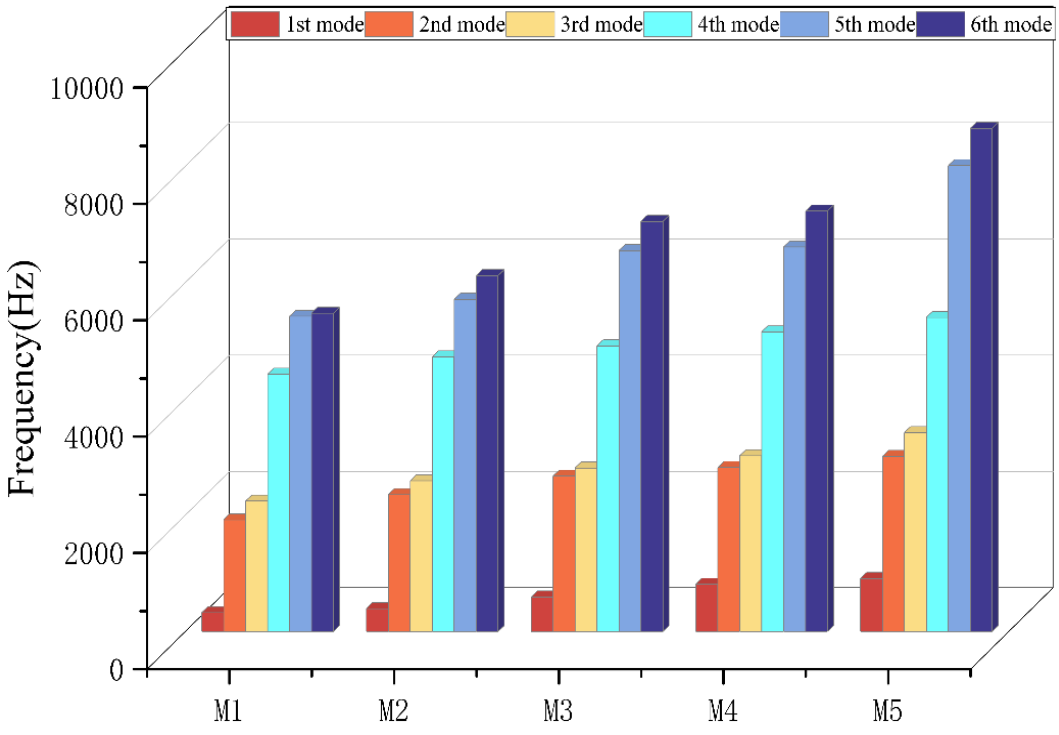

Figure 5. Results of the sixth-order mode.

In transient analysis, as shown in Figure 6, the maximum stress values of the crown, implant, and surrounding bone tissue within one cycle are presented. The results indicate that both the crown and implant of M1 exhibited the highest von Mises stresses, with a maximum stress of 93.048 MPa in the crown and 157.08 MPa in the implant, which were 18.1% and 7.4% higher than the results in static analysis. The crown and implant of M5 exhibited the lowest crown stress and implant von Mises stress values, at 35.265 and 69.909 MPa, respectively, which were 28.6% and 19.3% higher than the static results. Additionally, the maximum principal stresses in both cortical and cancellous bones were the highest in M1, with no significant differences among other groups. However, in the mandible, the cortical bone bears most of the stress distribution, with a maximum principal stress 4–5 times that of the cancellous bone. Most of the stress in the cortical bone is concentrated within the 3 mm region adjacent to the neck of the implant.

As shown in Figure 7, the static and dynamic simulation results exhibited similar patterns. However, the maximum equivalent stress in the dynamic simulation was 10%–30% higher than that in the static simulation, which is consistent with the experimental results reported by Alemayehu [19]. As shown in Figure 8, among the five stages of the dynamic loading cycle, the equivalent stress was the highest in Stage II, reaching its peak at 0.15 s, corresponding to the maximum chewing force. Regarding the equivalent stress of dental crown and implant, in all five experiments, the load gradually increased in Stage I, reached its peak at the end of Stage II, then decreased in Stage III due to shear forces after lateral sliding following anterior tooth cutting, and began to increase again in Stage IV. Finally, the stress gradually decreased when the occlusal force was released. The dynamic loading better simulated the stress distribution of the implant and surrounding bone tissue under masticatory force.

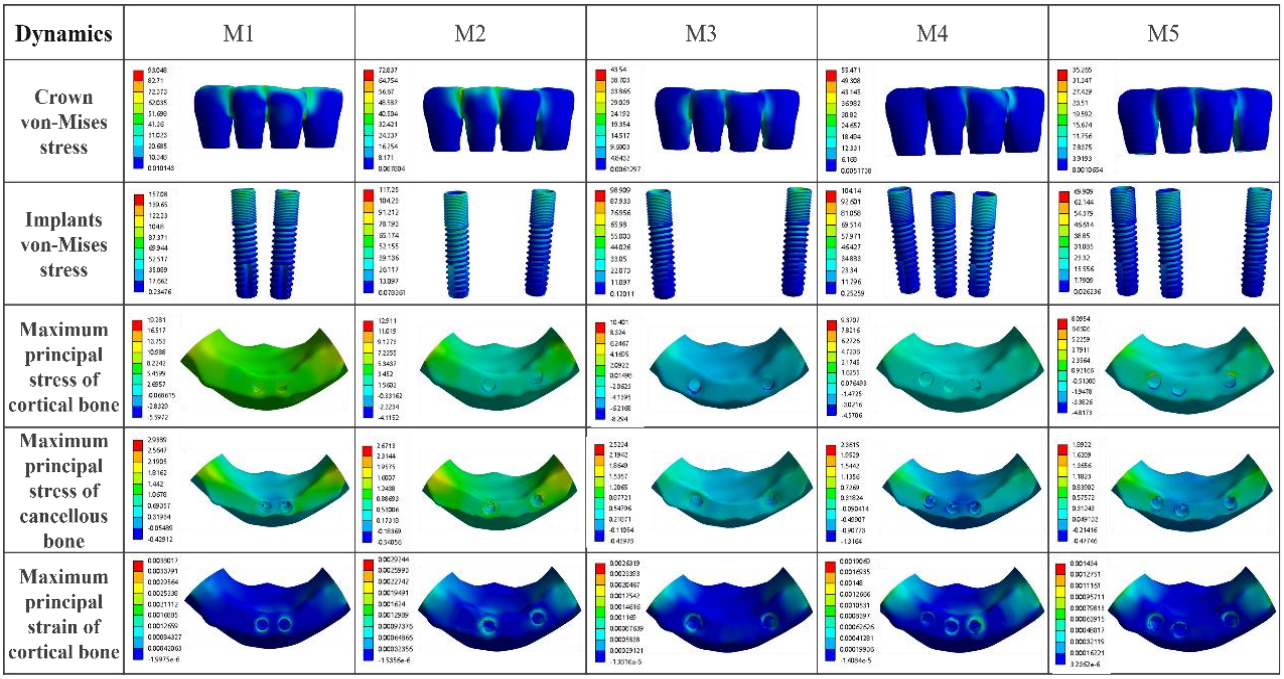

Figure 6. Representative screenshots of transient analysis results (crown and implants von Mises stress, maximum principal stress of cortical bone and cancellous bone, and maximum principal strain of cortical bone for M1–M5).

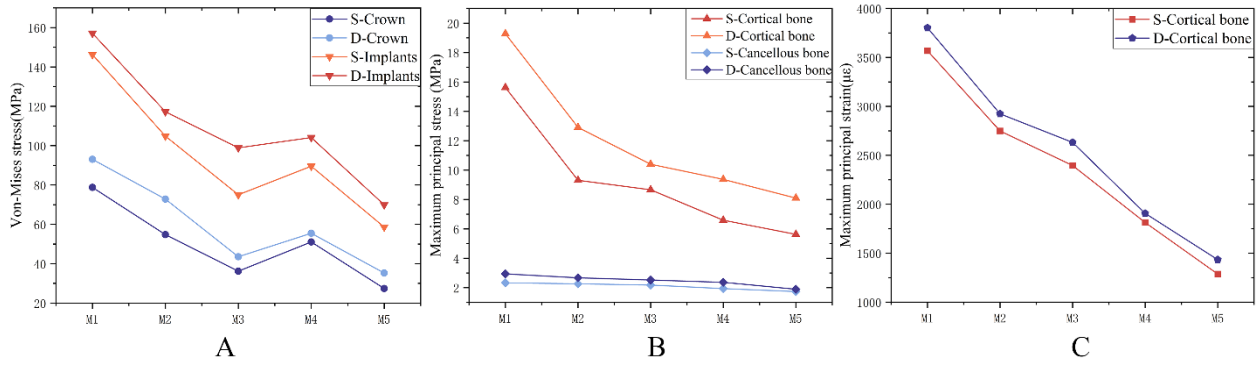

Figure 7. Comparison of static loading and dynamic loading results for M1–M5. A) Maximum von Mises stress of the crown and implant. B) Maximum principal stress in the cortical and cancellous bones. C) Maximum principal strain of the cortical bone.

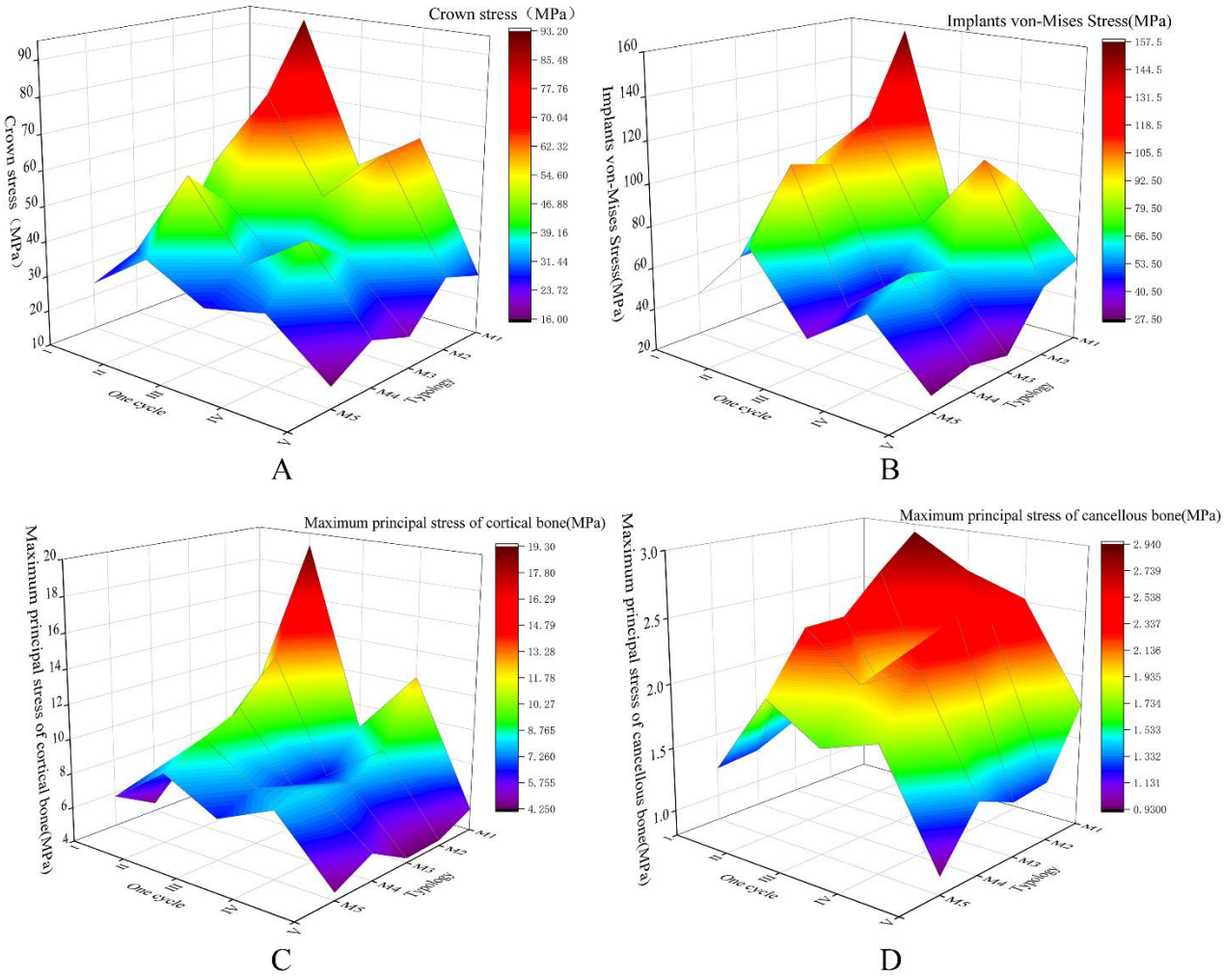

Figure 8. Results of dynamic loading at various stages for M1–M5. A) Crown von Mises stress. B) Implants von Mises stress. C) Maximum principal stress of the cortical bone. D) Maximum principal stress of the cancellous bone.

4. Discussion

Finite element analysis is a non-invasive mechanical method widely used in biomechanical research of oral implant restorations. Complex objects can be simplified to obtain approximate values by dividing the research objectives into a finite number of units and nodes and studying their mechanical properties, combined with the powerful computing power of the computer [30,31]. This simple, efficient, and economical method has become increasingly mature. Implant restoration plans are continuously optimized by simulating the complex oral environment in different situations and analyzing the related mechanical properties, thereby providing a reliable theoretical basis for personalized clinical restoration [32–34]. This paper compared and analyzed the biomechanical properties of five implant restoration options from the perspective of static loading and dynamic loading regarding the specific case of four missing incisors in the anterior mandibular region. The research results are of specific theoretical reference value for clinical practice.

Comparing the results of static and dynamic loading, the maximum von Mises stress of the implant was approximately twice that of the four-unit crown. The maximum equivalent stress values of the crowns relative to the implants in the five groups were ranked as follows: M1 > M2 > M4 > M3 > M5. The significant difference between the maximum and minimum equivalent stress values may be attributed to significant stress concentration in the design of cantilever bridges. The stress concentration occurs below the connection point of the cantilever end of the crown and in the neck region of the implant. The three-implant configuration reduced stress by approximately 50% compared with the two-implant configuration. Additionally, the stress in a fixed bridge supported by two implants is lower than that of a cantilever bridge supported by three implants, indicating significant stress concentration in cantilever bridges. In contrast, there is a more uniform stress distribution in a fixed bridge supported by three implants, demonstrating the optimal stress distribution performance.

According to Frost's minimum strain stimulus theory [26], specifically when the strain on bone tissue is lower than 100 με, the bone resorption rate exceeds the bone formation rate, resulting in bone resorption; when the strain is between 100 and 1500 με, the bone formation rate and resorption rate are roughly equal, maintaining normal bone quality and appropriately increasing it; when the strain is within the range of 1500–3000 μm, the bone plastic structure is activated, and bone stress promotes the growth of the bone tissue. Strain within the range of 3000 to 25,000 μm will cause damage to bone tissue. Under dynamic loading, the maximum principal strain in Group M1 was 3,802 με, causing damage to bone remodeling. In Group M5, the maximum principal strain was 1,434 με, ensuring normal bone quality. In Group M3, the maximum principal strain was 2,632 με, which is beneficial for promoting the growth of the bone tissue. A fixed bridge with two implants may be more advantageous than one with three implants under poor quality of the mandibular bone.

In modal analysis, the M5 group had the highest resonant frequency at 8653 Hz, nearly twice that of the M1 group. However, there was no significant overall difference between the M4 and M5 groups, as the three types of implants increased the contact area with bone tissue to enhance the stability of implant restoration [35]. The M1 group exhibited a double cantilever configuration and resulted in the lowest resonant frequency, which is attributed to the non-axial forces applied at the cantilever ends to generate the maximum bending moment at the implant position, making the double-end cantilever configuration the least effective for implant placement.

Researchers commonly use the finite element method of static loading in oral implant restorations, generating various results. Mitra et al. [36] used finite elements to study a total of six groups of models with three implant-abutment connection methods. Static analysis shows a better stress distribution of the platform-switching tapered abutment connection. Barbosa et al. [37] used finite element analysis to evaluate the stress of three NDI models and three ENDI (extra-narrow-diameter implant) models, showing high-stress concentrations of one-piece ENDIs under non-axial loads and favorable performance of NDIs. Despite the particular convenience of the simplified model using static loading, the inertial and damping effects of dynamic chewing force were overlooked, and only the response of the structure under steady-state conditions was analyzed. Due to the short stress phase of a single chewing cycle, a dynamic loading analysis is required to restore the real stress effect of chewing on the implant and surrounding bone [38]. The experimental results of Geramizadeh showed that the stress caused by dynamic loading was 10%–30% higher than that caused by static loading [39]. Through finite element analysis of the implant under static load, dynamic load, and fatigue behavior, Kayabassı et al. [40] also found that the stress under dynamic loading was 10%–20% higher than that under static loading.

As is well-known, the mandible has an outer layer of dense cortical bone and an inner layer of porous cancellous bone. The cancellous bone has a high vertical elastic modulus, which can resist the compressive stress caused by chewing. Horizontally, the cancellous bone can provide toughness through the interlaced arrangement of bone trabeculae to absorb lateral impact. Such a hierarchical structure can cope with loads from different directions as a result of its adaptation to complex mechanical environments [41,42]. Despite remarkable discoveries made by many scholars, the mandible is different in every way, and its complex internal structure and laws have not yet been thoroughly studied. Toniolo et al. [43] designed a computational model for the response of bone tissue to actual anisotropic bone structures. The elastic modulus distribution of orthotropic bone tissue can be measured through the combination of CT data and micro-mechanical modeling techniques. Zhu et al. [44] reported a magnetic micro-manipulation device and further extended the anisotropy evaluation method by determining the spatial heterogeneity of the mandible and the stiffness of each anisotropy through experiments on mice. This paper adopted orthogonal anisotropic material properties for the mandible and improved the simulation accuracy while ensuring computational efficiency through directional characteristics and parameter reduction, thereby enhancing the credibility of the results.

Through experimental results, similar phenomena exist at the connection between the crown and the bridge, in addition to significant stress concentration at the implant neck, making it meaningful to change the connection structure of the crown and bridge while ensuring the aesthetic appearance of the implant. Jwalithaclare et al. [45] conducted a finite element analysis of a model of a 4-unit crown bridge with three different materials and three different bridge connectors, showing better fracture resistance of the design targeting the circular connector. Reimann et al. [46] studied the influence of four different crown-bridge connection cross-sections on bridge strength using finite element analysis and found that the bridge deflection depends on the cross-section of the connector and the elastic modulus of the selected material. Huang et al. [47] performed finite element analysis on three implant abutment designs and two connectors, showing that a rigidly connected prosthesis can be used with a three-body abutment at a distance of 12 mm between the implant and the natural tooth. The design of the structure at the connection of the multi-unit bridge has positive significance for implant restoration in patients with multiple tooth loss or edentulous jaws.

Another noteworthy point lies in the fact that, in this experiment, the double-end cantilever bridge supported by two NDIs exhibited large stress concentrations at the cantilever end; the same was true for the single-end cantilever bridge. Such stress concentration had a significant impact compared with the fixed bridge design, and its maximum equivalent stress was almost twice that of the fixed bridge design. However, it is undeniable that the design of the cantilever bridge remains optimistically valuable. On the one hand, it further lowers the cost and complexity of surgery by reducing the use of implants. On the other hand, it brings positive value by finding a better implant material through the optimization of the structural topology of stress concentration sites to improve stress concentration. Colep´ıcolo et al. [48] designed a new type of double-parabolic abutment with an implant located between two unit bridges. Such an innovative design has a more dispersed stress distribution than the traditional cantilever bridge. Regardless of the repair method used, the stress generated is much lower than the yield strength of the material, indicating that cantilever bridge implants remain advantageous under poor quality of the mandible.

The basic assumptions used in this experiment were continuity, linear elasticity, and isotropy. However, due to the complexity of the real oral environment, the consideration of jawbone orthotropy remains insufficient. The impact of periodontal ligaments on implants must also incorporate viscoelasticity and superelasticity, among others. Also, the aging and creep effects of the cement layer are commonly ignored. Moreover, even the impact of load on the stability of the implant must be evaluated at the microscale [49]. Further investigation should focus on the heterogeneities of the mandible. Since the mechanism of trabecular heterogeneity covers multiple disciplines, interdisciplinary cooperation and technological innovation are necessary to achieve precise regulation. The real loading force is time-varying and multidirectional, while the chewing force in the experiment is assumed to be simplified and fails to reflect actual physiological fluctuations. It is insufficient to carry out transient analysis using dynamic loading, and only mechanical effects are considered. In actual oral chewing, the oral environment involves coupled thermal-mechanical-chemical field effects, and the mechanism of action remains unclear. Future development of finite element technology will be able to more realistically simulate the actual environment, effectively reduce the stress distribution of the implant through the study of gradient materials, and improve stress concentration by optimizing structural parameters, so as to achieve more reliable results of finite element [50].

5. Conclusion

In the case of four missing incisors in the mandibular anterior region, a fixed bridge restoration supported by three NDIs exhibits the optimal results. Cantilever bridge restorations should be used with caution since they are prone to stress concentrations at the junction of the implant neck and crown bridge. However, the maximum equivalent force generated by the cantilever bridge design is still far less than the yield strength of the material, which is advantageous in anatomical constraint regions. In addition, finite element dynamic loading brings about an overall stress 10%–30% higher than static loading. Finite element techniques have limitations at the current stage. Since the real oral environment involves coupled thermal-force-chemical multi-field effects, further investigation should focus on multi-physical field coupling models to simulate more realistic environments. Finite element analysis techniques will achieve extensive application in the field of oral implantology.

Use of AI tools declaration

The authors declare they have not used Artificial Intelligence (AI) tools in the creation of this article.

Acknowledgments

This work is supported by the Science and Technology Commission of Shanghai Municipality, Science, Technology and Innovation Action Plan (grant numbers: 23141901400), Collaborative Innovation Fund of Shanghai Institute of Technology (grant numbers: XTCX2023−18), Science and Technology Development Fund of Shanghai Institute of Technology (grant numbers: KJFZ2024-17).

Conflict of interest

The authors declare no conflict of interest.

Author contributions

Song Huang: manuscript editing, 3D modeling and simulation experiments; Jianguo Zhang: project analysis, review and editing, securing funding. Xiaoying Zhang: resource search, experimental evaluation. Fengling Hu and Youcheng Yu: paper revision and optimization.

Ethics approval and consent to participate

Approved was obtained from the Medical Ethics Committee of Zhongshan Hospital, Fudan University (approval number B2024-068R). The procedures used in this study adhere to the tenets of the Declaration of Helsinki.

References

1. Ma M, Qi M, Zhang D, et al. (2019) The clinical performance of narrow diameter implants versus regular diameter implants: a meta-analysis. *J Oral Implantol* 45: 503–508. https://doi.org/10.1563/aaid-joi-D-19-00025
2. Gao J, Pan Y, Gao Y, et al. (2024) Research progress on the preparation process and material structure of 3D-printed dental implants and their clinical applications. *Coatings* 14: 781. https://doi.org/10.3390/coatings14070781
3. Ahn JH, Lim YJ, Lee J, et al. (2024) A one-year randomized controlled clinical trial of three types of narrow-diameter implants for fixed partial implant-supported prosthesis in the mandibular incisor area. *Bioengineering* 11: 272. https://doi.org/10.3390/bioengineering11030272
4. Telles LH, Portella FF, Rivaldo EG (2019) Longevity and marginal bone loss of narrow-diameter implants supporting single crowns: a systematic review. *PLoS One* 14: e0225046. https://doi.org/10.1371/journal.pone.0225046

5. Gonzalez-Valls G, Roca-Millan E, Céspedes-Sánchez JM, et al. (2021) Narrow diameter dental implants as an alternative treatment for atrophic alveolar ridges. Systematic review and meta-analysis. *Materials* 14: 3234. https://doi.org/10.3390/ma14123234
6. Antiua E, Escuer V, Alkhraisat MH (2022) Short narrow dental implants versus long narrow dental implants in fixed prostheses: a prospective clinical study. *Dent J* 10: 39. https://doi.org/10.3390/dj10030039
7. Kim JE, Yoon Y, Pae A, et al. (2023) Clinical outcome of narrow diameter dental implants: a 3-year retrospective study. *Max Plast Reconstr S* 45: 26. https://doi.org/10.1186/s40902-023-00394-6
8. Zhang S, Wang W, Cao Q, et al. (2023) Three-dimensional finite element stress analysis of different implant-supported bridges in the maxillary incisal regions. *J Med Biol Eng* 43: 322–331. https://doi.org/10.1007/s40846-023-00795-y
9. Valera-Jiménez JF, Burgueño-Barris G, Gómez-González S, et al. (2020) Finite element analysis of narrow dental implants. *Dent Mater* 36: 927–935. https://doi.org/10.1016/j.dental.2020.04.013
10. Sadek HS, Anany NM, Diab AH, et al. (2025) Biomechanical evaluation of cantilevered 2-Unit implant-supported prostheses: a 3D finite element study. *Int Dent J* 75: 1913–1920. https://doi.org/10.1016/j.identj.2025.01.014
11. Kondo Y, Sakai K, Minakuchi H, et al. (2024) Implant-supported fixed prostheses with cantilever: a systematic review and meta-analysis. *Int J Implant Dent* 10: 57. https://doi.org/10.1186/s40729-024-00573-8
12. Deste Gökay G, Oyar P, Gökçimen G, et al. (2024) Static and dynamic stress analysis of different crown materials on a titanium base abutment in an implant-supported single crown: a 3D finite element analysis. *BMC Oral Health* 24: 545. https://doi.org/10.1186/s12903-024-04328-0
13. Alrabiah M (2019) Comparison of survival rate and crestal bone loss of narrow diameter dental implants versus regular dental implants: a systematic review and meta-analysis. *J Investig Clin Dent* 10: e12367. https://doi.org/10.1111/jicd.12367
14. Bielemann AM, Marcello-Machado RM, Schuster AJ, et al. (2019) Healing differences in narrow diameter implants submitted to immediate and conventional loading in mandibular overdentures: a randomized clinical trial. *J Periodontal Res* 54: 241–250. https://doi.org/10.1111/jre.12624
15. Shihab T, Muhsin SA, Al Marza R (2025) Cantilever extension for implant-supported fixed dental prostheses: a systematic review. *Iraqi J Med Health Sci* 2: 8–16. https://doi.org/10.51173/ijmhs.v2i1.3
16. Zhang X (2013) Evaluation of the therapeutic efficiency of mandibular anterior implant-supported fixed bridges with cantilevers. *Chin Med J* 126: 4665–4669. https://doi.org/10.3760/cma.j.issn.0366-6999.20131291
17. De Stefano M, Lanza A, Sbordone L, et al. (2023) Stress-strain and fatigue life numerical evaluation of two different dental implants considering isotropic and anisotropic human jaw. *Proc Inst Mech Eng Part H* 237: 1190–1201. https://doi.org/10.1177/09544119231193879
18. Falcinelli C, Valente F, Vasta M, et al. (2023) Finite element analysis in implant dentistry: state of the art and future directions. *Dent Mater* 39: 539–556. https://doi.org/10.1016/j.dental.2023.04.002

19. Alemayehu DB, Jeng YR (2021) Three-dimensional finite element investigation into effects of implant thread design and loading rate on stress distribution in dental implants and anisotropic bone. *Materials* 14: 6974. https://doi.org/10.3390/ma14226974
20. Zhang JG, Hou H, Chen P, et al. (2024) Biomechanical performance of different implant spacings and placement angles in partial fixed denture prosthesis restorations: a finite element analysis. *J Med Biol Eng* 44: 685–695. https://doi.org/10.1007/s40846-024-00896-2
21. Barao VA, Assuncao WG, Tabata LF, et al. (2008) Effect of different mucosa thickness and resiliency on stress distribution of implant-retained overdentures-2D FEA. *Comput Methods Programs Biomed* 92: 213–223. https://doi.org/10.1016/j.cmpb.2008.07.009
22. Cicciù M, Cervino G, Terranova A, et al. (2019) Prosthetic and mechanical parameters of the facial bone under the load of different dental implant shapes: a parametric study. *Prosthesis* 1: 41–53. https://doi.org/10.3390/prosthesis1010006
23. Hosseini-Faradonbeh SA, Katoozian HR (2022) Biomechanical evaluations of the long-term stability of dental implant using finite element modeling method: a systematic review. *J Adv Prosthodont* 14: 182–202. https://doi.org/10.4047/jap.2022.14.3.182
24. Sahin Hazir D, Sozen Yanik I, Guncu MB, et al. (2025) Biomechanical behavior of titanium, cobalt-chromium, zirconia, and PEEK frameworks in implant-supported prostheses: a dynamic finite element analysis. *BMC Oral Health* 25: 97. https://doi.org/10.1186/s12903-025-05486-5
25. Fiorillo L, Cicciu M, D'Amico C, et al. (2020) Finite element method and von mises investigation on bone response to dynamic stress with a novel conical dental implant connection. *Biomed Res Int* 2020: 2976067. https://doi.org/10.1155/2020/2976067
26. Frost HM (2004) A 2003 update of bone physiology and Wolff's Law for clinicians. *The Angle Orthodontist* 74: 3–15. https://doi.org/10.1043/0003-3219
27. Yemineni BC, Mahendra J, Nasina J, et al. (2020) Evaluation of maximum principal stress, von mises stress, and deformation on surrounding mandibular bone during insertion of an implant: a three-dimensional finite element study. *Cureus* 12: e9430. https://doi.org/10.7759/cureus.9430
28. Martinez S, Lenz J, Schweizerhof K, et al. (2015) A variable finite element model of the overall human masticatory system for evaluation of stress distributions during biting and bruxism. *In10th European LS-DYNA Conference,* Würzburg, Germany. 2015. https://doi.org/10.1201/b17071-3
29. Martinez S, Lenz J, Schindler H, et al. (2021) Clinical data-driven finite element analysis of the kinetics of chewing cycles in order to optimize occlusal reconstructions. *Cmes-Comp Model Eng* 129: 1259–1281. https://doi.org/10.32604/cmes.2021.017422
30. Roatesi I, Roatesi S (2023) Biomechanics study of dental implant-bone system by finite element method. *J Braz Soc Mech Sci Eng* 45: 345. https://doi.org/10.1007/s40430-023-04170-5
31. Xu Y, Fan Y, Xu G (2023) Progress of finite element analysis method for oral implantology. *Acad J Med Health Sci* 4: 65–70. https://doi.org/10.25236/ajmhs.2023.040811
32. Lisiak-Myszke M, Marciniak D, Bielinski M, et al. (2020) Application of finite element analysis in oral and maxillofacial surgery-a literature review. *Materials* 13: 3063. https://doi.org/10.3390/ma13143063
33. Manea A, Bran S, Dinu C, et al. (2019) Principles of biomechanics in oral implantology. *Med Pharm Rep* 92: S14–S19. https://doi.org/10.15386/mpr-1512
34. Wang CX, Rong QG, Zhu N, et al. (2023) Finite element analysis of stress in oral mucosa and titanium mesh interface. *Bmc Oral Health* 23: 25. https://doi.org/10.1186/s12903-022-02703-3

35. Nienkemper M, Wilmes B, Pauls A (2013) Impact of mini-implant length on stability at the initial healing period : a controlled clinical study. *Head Face Med* 9: 30. https://doi.org/10.1186/1746-160X-9-30
36. Mitra D, Gurav P, Rodrigues S, et al. (2023) Evaluation of stress distribution in and around dental implants using three different implant-abutment interfaces with platform-switched and non-platform-switched abutments: a three-dimensional finite element analysis. *J Dent Res Dent Clin Dent Prospects* 17: 256–264. https://doi.org/10.34172/joddd.2023.40723
37. Barbosa FT, Zanatta LCS, de Souza Rendohl E, et al. (2021) Comparative analysis of stress distribution in one-piece and two-piece implants with narrow and extra-narrow diameters: a finite element study. *PLoS One* 16: e0245800. https://doi.org/10.1371/journal.pone.0245800
38. Martinez Choy SE, Lenz J, Schweizerhof K, et al. (2017) Realistic kinetic loading of the jaw system during single chewing cycles: a finite element study. *J Oral Rehabil* 44: 375–384. https://doi.org/10.1111/joor.12501
39. Geramizadeh M, Katoozian H, Amid R, et al. (2017) Finite element analysis of dental implants with and without microthreads under static and dynamic loading. *J Long Term Eff Med Implants* 27: 25–35. https://doi.org/10.1615/JLongTermEffMedImplants.2017020007
40. Kayabaşı O, Yüzbasıoğlu E, Erzincanlı F (2006) Static, dynamic and fatigue behaviors of dental implant using finite element method. *Adv Eng Softw* 37: 649–658. https://doi.org/10.1016/j.advengsoft.2006.02.004
41. Cicciu M, Cervino G, Milone D, et al. (2018) FEM investigation of the stress distribution over mandibular bone due to screwed overdenture positioned on dental implants. *Materials* 11: 1512. https://doi.org/10.3390/ma11091512
42. Marcián P, Wolff J, Horácková L, et al. (2018) Micro finite element analysis of dental implants under different loading conditions. *Comput Biol Med* 96: 157–165. https://doi.org/10.1016/j.compbiomed.2018.03.012
43. Toniolo I, Salmaso C, Bruno G, et al. (2020) Anisotropic computational modelling of bony structures from CT data: an almost automatic procedure. *Comp Meth Prog Bio* 189: 105319. https://doi.org/10.1016/j.cmpb.2020.105319
44. Zhu M, Zhang KW, Tao H, et al. (2020) Magnetic micromanipulation for measurement of stiffness heterogeneity and anisotropy in the mouse mandibular arch. *Research* 2020: 7914074. https://doi.org/10.34133/2020/7914074
45. Jwalithaclare M, Kumar CHS, mondal S (2024) A comparative evaluation of the effect of three different connector designs in predicting fracture resistance of metallic, metal-ceramic and all-ceramic core full coverage four unit bridge: a finite element analysis. *TWIST* 19: 195–200. https://doi.org/10.5281/zenodo.10049652#327
46. Reimann L, Zmudzki J, Dobrzanski LA (2015) Strength analysis of a three-unit dental bridge framework with the finite element method. *Acta Bioeng Biomech* 17: 51–59. https://doi.org/10.5277/Abb-00091-2014-02
47. Huang LS, Huang YC, Yuan CD, et al. (2023) Biomechanical evaluation of bridge span with three implant abutment designs and two connectors for tooth-implant supported prosthesis: a finite element analysis. *J Dent Sci* 18: 248–263. https://doi.org/10.1016/j.jds.2022.05.026
48. Colepícolo LS, Magalhães PHV, Martinez MAM, et al. (2025) Comparative analysis of a conventional cantilever abutment and innovative double abutment in dental implant prosthesis: a finite element analysis study. *Biomed Eng Adv* 9: 100151. https://doi.org/10.1016/j.bea.2025.100151

49. Gu JY, Ke ZW, Pan H, et al. (2025) Hierarchical engineering scaffolds for oral and craniofacial tissue regeneration: recent advances and challenges. *Appl Mater Today* 42: 102546. https://doi.org/10.1016/j.apmt.2024.102546
50. Lahoud P, Faghihian H, Richert R, et al. (2024) Finite element models: a road to in-silico modeling in the age of personalized dentistry. *J Dent* 150: 105348. https://doi.org/10.1016/j.jdent.2024.105348

AIMS Press